CFD Letters

Journal homepage:
https://semarakilmu.com.my/journals/index.php/CFD_Letters/index
ISSN: 2180-1363

CFD Analysis into the Breakdown of Catamaran Resistance Based on the Original Formula by Insel and Molland

Amalia Ika Wulandari[1], Aries Sulisetyono[2], I Ketut Aria Pria Utama[2,*]

[1] Department of Ocean Engineering, Faculty of Marine Technology, Institut Teknologi Sepuluh Nopember (ITS), Surabaya, Indonesia
[2] Department of Naval Architecture, Faculty of Marine Technology, Institut Teknologi Sepuluh Nopember (ITS), Surabaya, Indonesia

ARTICLE INFO

Article history:
Received 19 August 2024
Received in revised form 21 September 2024
Accepted 26 October 2024
Available online 30 November 2024

Keywords:
Resistance; warship; CFD; Catamaran

ABSTRACT

Over the last 40 years, the use of fast catamaran has progressively developed attributed to its unique characteristics on resistance and seakeeping. The advantages have also been applied to military vessels to gain both resistance and seakeeping benefits. The current study focuses on the resistance of catamaran warships to provide less resistance, therefore, the size of engine and emission of toxic gases to the atmosphere. The total resistance of a catamaran will be different from a monohull of equal displacement. There are several factors including viscous interference factors such as ϕ, which is introduced to take account of the pressure field change around the hull, σ takes account of the velocity augmentation between the two hulls and calculated from an integration of local frictional resistance over the wetted surface, and τ is the wave resistance interference factor change. Those resistance components were developed by Insel and Molland in the 1990s. The investigation discusses the derivation of those components numerically using Computational Fluid Dynamics (CFD) approach. The speeds (hence, the Froude numbers) are varied from 0.2 to 0.6 and the separations between the hulls (S/L) are made between 0.2 and 0.4 so the comparative purposes can be done against the classical work of Insel and Molland and other published data.

1. Introduction

The utilization of catamarans instead of the more traditional monohull high-speed vessels is growing in various fields such as transportation, naval operations, and offshore applications [1]. This upward trend is a direct result of the global demand for vessels that are both commercially and militarily efficient, providing high speed, the potential for better performance in rough seas, lower hydrodynamic resistance in waves, and a more usable deck area. Achieving improved seakeeping and other hydrodynamic performance greatly depends on the design and hull geometry of catamarans. The design and shape of catamarans play a crucial role in enhancing their performance at sea, particularly in terms of seakeeping and hydrodynamics. Catamarans have gained popularity as a mode of transportation because they offer a wider deck area, increased stability, and a more

* *Corresponding author.*
E-mail address: kutama@its.ac.id (I Ketut Aria Pria Utama)

https://doi.org/10.37934/cfdl.17.5.103119

comfortable and safe experience for passengers [1,2]. The catamaran (double hull) tends to have a more draft lower than monohull ships with the same displacement, thus it can be operated in shallow water [3]. The resistance component of the catamaran has more complex phenomena compared to the monohull, because of the interaction effect between two hulls and this creates interference of viscous and wave resistance components [4,5].

Barrier viscous interferences arise when the uneven flow of water around the hull disrupts the formation of the boundary layer and longitudinal vortices. This is further complicated by wave interference, which is the result of the interaction of waves created by each individual catamaran hull. Several factors play a role in this, including viscous interference factors like ϕ, which is introduced to consider changes in the pressure field around the hull, σ, which accounts for the increase in velocity between the two hulls and is calculated by integrating local frictional resistance over the wetted surface, and τ, which represents changes in wave resistance interference factors. The analysis of these catamaran components has been carried out by Jamaluddin *et al.,* [5] and Insel and Molland [6].

This present study research about component resistance of catamaran in asymmetrical hull and compare with previous study. The investigation discusses the derivation of those components numerically using Computational Fluid Dynamics (CFD) approach [5,7,8]. In a general context, this computational approach exhibits favorable agreement with the outcomes of experimental model tests conducted in the towing tank, as evidenced by the studies of He *et al.,* [9], Sadeghi and Hajivand [10], and Sadeghi and Zeraatgar [11]. The speeds (therefore, the Froude numbers) are varied from 0.2 to 0.7 and the separations between the hulls (S/L) are made between 0.2 and 0.4, hence, the comparative purposes can be done against the classical work of Insel and Molland and other published data. Those previous studies mentioned above resistance component still rarely conducted (σ, ø and τ). This study conducted previously by Jamaluddin *et al.,* [5] and Insel and Molland [6]. However, the study involves a catamaran hull and investigates how different hull separations and speed variations impact its performance. Two distinct interference effects were identified as contributing to the overall resistance: Viscous interference, which results from the uneven flow around the demi-hulls, influencing the formation of the boundary layer. Wave interference, stemming from the interaction between the wave systems generated by each demihull. This study employed CFD-based software and applied the incompressible unsteady Reynolds-Averaged Navier Stokes equations (RANS) for modeling. to handle nonlinear free surface conditions iturbulent flow, the research used the Volume of Fluid (VOF) method to discretize the RANSE and continuity equations. The chosen turbulence model was the SST k-ω (Shear-Stress Transport for k-ω) model, which is integrated into the ISIS-CFD solver code. In this context, 'k' represents turbulent kinetic energy, and 'ω' stands for the specific dissipation rate [12].

2. Methodology

2.1 The Catamaran Warship

The object of this research is a warship catamaran with length of 16.52 m, breadth of 6.649 m, draft of 1.184 m, and speed of 40 knots. The test is carried out numerically with a variation of speed (Froude Number) between 0.2 and 0.7 and separation to length (S/L) ratios 0.2, 0.3 and 0.4.

2.2 Numerical Equation

In this latest research, a readily available viscous solver was used to tackle the unsteady Reynolds-Averaged Navier-Stokes (URANS) equations, which are described in previous studies [7,8]. The core equations that govern this study, which include the continuity and momentum equations, were discretized using the finite volume method (FVM) as detailed in previous studies [13,14]. Specifically, the continuity and momentum equation can be represented in Eq. (1) and Eq. (2) as follows

$$\frac{\partial(\rho\bar{u}_i)}{\partial x_i} = 0 \tag{1}$$

$$\frac{\partial(\rho\bar{u}_i)}{\partial t} + \frac{\partial}{\partial x_j}\left(\rho\overline{u_\iota u_J} + \rho\overline{u'_\iota u'_J}\right) = -\frac{\partial\bar{p}}{\partial x_i} + \frac{\partial\overline{\tau_{\iota J}}}{\partial x_j} = 0 \tag{2}$$

where ρ is the fluid density, x_i and x_j are the components of the position vector in Cartesian coordinate, $\bar{u}_i$ and $\bar{u}_j$ are the components of the mean velocity vector, $\overline{u'_\iota u'_J}$ is the Reynolds stresses and $\bar{p}$ is the mean pressure. $\overline{\tau_{\iota J}}$ are the components of the mean viscous stress tensor, which can be written in Eq. (3).

$$\overline{\tau_{\iota J}} = \mu\left(\frac{\partial\overline{u_\iota}}{\partial x_j} + \frac{\partial\overline{u_J}}{\partial x_i}\right) \tag{3}$$

where μ is the fluid dynamic viscosity. The k −ω SST turbulence model, which has been widely used for marine hydrodynamics is employed as shown in Eq. (4) [15].

$$\frac{\gamma}{v_t}P - \beta\rho\omega^2 + \frac{\partial}{\partial_{xj}}\left[(\mu + \sigma_\omega\mu_t)\frac{\partial_\omega}{\partial_{xj}}\right] + 2(1 - F_1)2\rho_{\omega 2}\frac{1}{\omega}\frac{\partial_k}{\partial_{xj}}\frac{\partial_\omega}{\partial_{xj}} - \left(\frac{\partial(\rho\omega)}{\partial_t} + \frac{\partial(\rho uj\omega)}{\partial_{xj}}\right) = 0 \tag{4}$$

The symbols in the equation likely represent various parameters and variables in fluid mechanics or turbulence modeling: γ for a specific ratio, v_t for turbulent viscosity, P for turbulence production, β for a turbulence model coefficient, ρ for fluid density, ω for specific dissipation rate, $\frac{\partial}{\partial_{xj}}$ for partial derivatives with respect to spatial coordinates, μ for dynamic viscosity σ_ω for a coefficient in the k-ω model, μ_t for turbulent viscosity, F_1 for a blending function,k for turbulent kinetic energy, $\frac{\partial_k}{\partial_{xj}}$ and $\frac{\partial_\omega}{\partial_{xj}}$ for partial derivatives of k and ω, $\frac{\partial(\rho\omega)}{\partial_t}$ for the time derivative of density times specific dissipation rate, and $\frac{\partial(\rho uj\omega)}{\partial_{xj}}$ for the partial derivative of density times velocity times specific dissipation rate with respect to spatial coordinates.

The principle particular of catamaran is shown in Table 1. The lines plan of catamaran as shown in Figure 1.

Table 1
Principle Particular of Catamaran

Parameter	Catamaran
Lwl (m)	16.52
B (m)	6.649
T (m)	1.184
Cb	0.319
Displ. (ton)	42.52
V (knot)	40

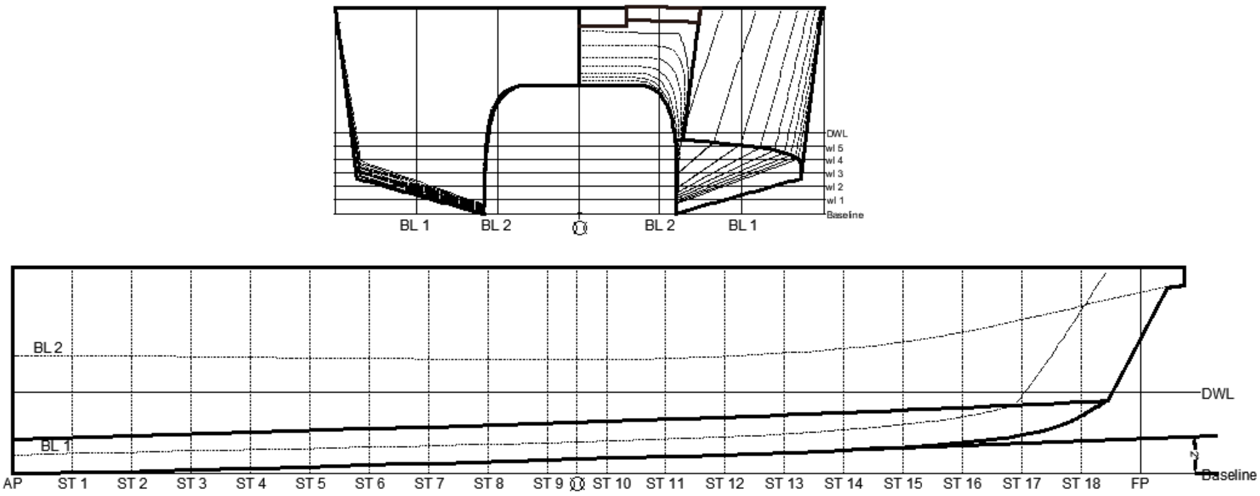

Fig. 1. Lines plan of catamaran

2.3 Resistance of Catamaran

The total resistance is analyzed in calm water with variation of speeds [6,16]. The total resistance of catamaran, in coefficient form may be expressed in Eq. (5) as:

$$C_{Tcat} = (1 + \emptyset k)\sigma C_F + \tau C_w \quad (5)$$

where

C_T = Total Resistance
C_F = Friction Resistance
C_w = Wave Resistance
$\emptyset$ = Factor for pressure field change
σ = velocity augmentation between the hulls
τ = Wave-resistance interference factor

The variable ø was introduced to account for changes in the pressure distribution around the half-hulls, while σ considers the velocity increase between the two hulls. The value of σ can be calculated by integrating the local frictional resistance across the wetted surface. Furthermore, the term (1+ k) represents the shape factor for the half-hull when it is analyzed independently. To enhance practical usability, Eq. (6) was reformulated in the following manner.

$$(C_T)_{CAT} = (1 + \beta k)C_F + \tau C_W \quad (6)$$

For practical purposes, ø and σ are combined into a viscous interference factor (β) in Eq. (7), where [6]

$$\beta = \frac{FF_{Cat} - 1}{FF_{Demi} - 1} \quad (7)$$

where FF_{Demi} is the form factor of the demihull = (1+k) and FF_{Cat} is the form factor of the catamaran = (1+βk).

The factor τ is wave interference and can be calculated from the Eq. (8).

$$\tau = \frac{C_{WCAT}}{C_{WDEMI}} = \frac{[C_T - (1+\beta k)C_F]_{CAT}}{[C_T - (1+k)C_F]_{DEMI}} \quad (8)$$

The value of the interference factor of the resistance component for the catamaran hull to the variation in the change in the distance between the hulls (S/L) and speeds is calculated based on the Eq. (9) and Eq. (10) below

$$IF_{Cv} = \frac{C_{Vcat}}{C_{Vdemi}} \quad (9)$$

$$IF_{Cw} = \frac{C_{wcat}}{C_{wdemi}} \quad (10)$$

The desire to break down the various components of resistance has driven efforts to employ Computational Fluid Dynamics (CFD) tools for estimating and predicting the flow characteristics around ship hulls, particularly in the context of resistance [18]. Some research has already been conducted in the maritime field in this regard [19]. However, there still exist uncertainties when it comes to computing viscous and wave resistances separately. This can be attributed to the shortcomings in modeling free surfaces during those earlier phases. Fortunately, modern CFD codes now incorporate improved free surface algorithms [20]. Consequently, our current research is centered on advancing free surface modeling while also considering the breakdown of ship resistance components, with a specific focus on catamaran resistance in this case.

2.4 Grid Independence Study

A grid independence study is a process in CFD where the solution of a CFD problem is tested to ensure that it is independent of the size of the grid used [17]. The research involves solving the identical problem using various grid sizes, spanning from coarse to fine, and then comparing the outcomes. It's essential that the finest grid produced is sufficiently fine to confirm that the CFD results obtained are considered as fully converged results. This investigation holds significance because it ensures the accuracy and dependability of the results obtained through CFD simulation. Table 2 presents the findings of a grid independence study for this particular model. According to the research by Molland and others, grid independence is achieved when the difference in resistance between a given number of elements and the preceding element is less than 2% [15]. In this study, the number of mesh elements was made between 619,530 and 4,615,990. According to Table 2 and Figure 2, the optimum number of grids are 2,920,594, satisfying the grid independence criteria.

Table 2
Grid Independence

Number of Grid	C_T (x 10^{-3})	Margin (%)
619,530	3.093	-
1,556,716	2.066	20%
1,945,586	1.971	2.34%
2,920,594	1.926	1.15%
3,258,389	1.906	0.53%
4,615,990	1.887	0.48%

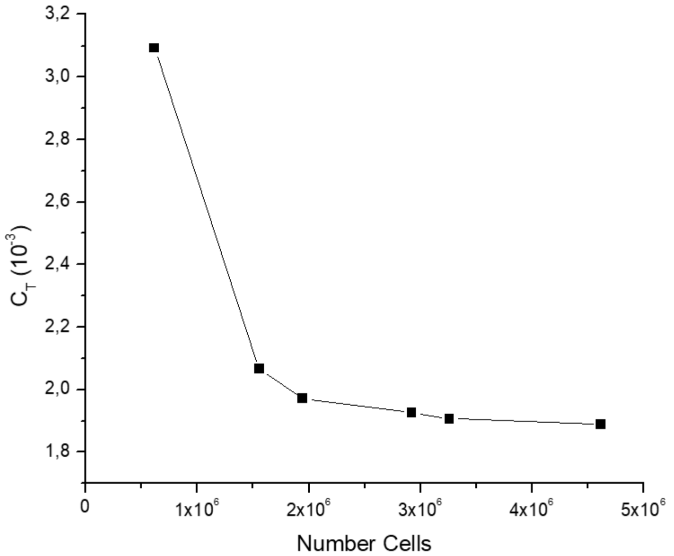

Fig. 2. Grid independence study of the different number of cells

2.5 Computational Model

Numerical simulations were performed for the warship models. CFD approach involves employing computer-based numerical simulation methods to replicate and examine problems in fluid mechanics [18]. The computational domain of the boundary conditions is outlined as follows: the entrance is set as velocity inlet, the exit as pressure outlet, both sides of the domain are labelled as symmetry planes, the top and bottom are designated as velocity inlets, and the surface of the ship is identified as a sliding wall, as shown in Figure 3.

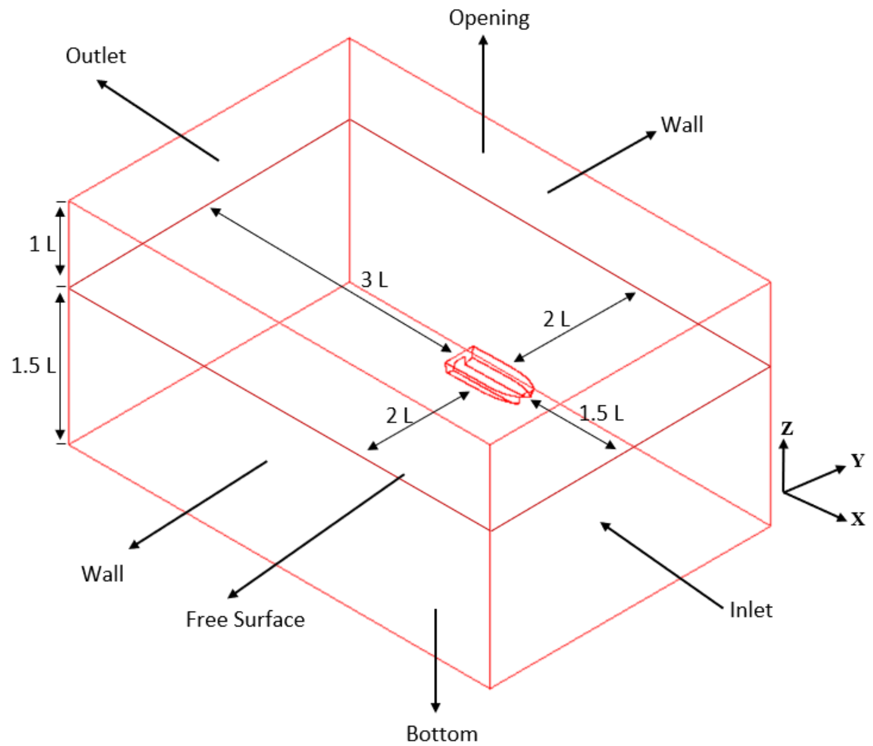

Fig. 3. Domain setting on CFD

The computational domain is partitioned into grid cells. To minimize grid density, typically, a larger grid size is employed for the surrounding domain, with finer grid cells concentrated around the hull. Additionally, the mesh for the free liquid surface is refined in the z-axis direction, and a specific mesh is established for the ship's surface. This is primarily done to control mesh thickness and adjust the wall distance represented as y+ value. The outcome of this meshing process is shown in Figure 4.

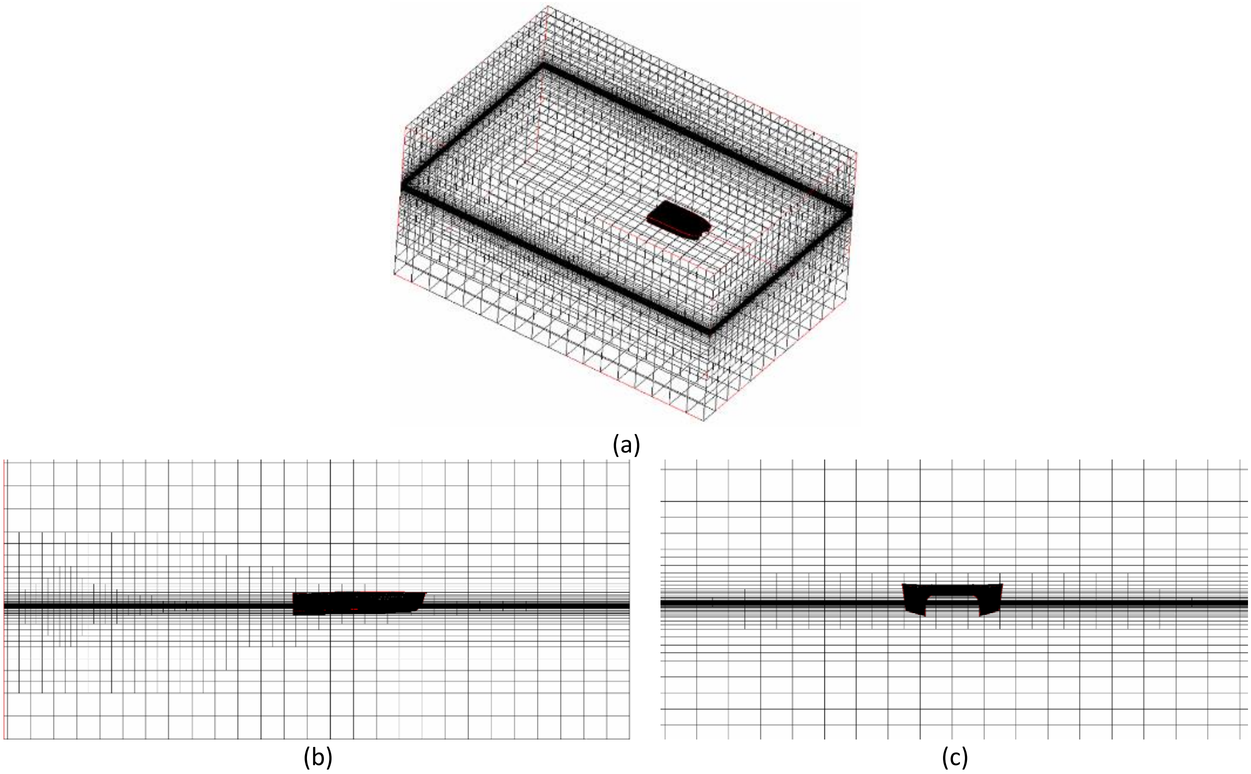

Fig. 4. Visualization meshing condition of ship; (a) Meshing in fluid domain with refinement levels, (b) Side view of Model, (c) Front View of Model

3. Result and Discussion

Using CFD software, the three-dimensional ship model was used to calculate the total resistance of variations of hull and variation of speed. with different hull spacing ratios S/L 0.2, 0.3, and 0,4 when the Froude Number (Fr) 0.2 to 0.7. the contour map of the numerical simulation showed in Figure 5(a) to Figure 5(f).

Figure 5(a) to Figure 5(f) illustrate variations in wave elevation based on different hull spacings and speeds, with a focus on Froude numbers (Fr). The image employs a colour scheme to depict wave heights surrounding the catamaran. Red hues denote elevated areas, while blue shades represent lower elevations. This colour scheme aids in comprehending how the catamaran influences the water surface. By measuring wave heights at specific locations within the image, it is possible to conduct a quantitative assessment of the catamaran's hydrodynamic performance across different scenarios. At Fr 0.2, the wave elevation is 1.45 m, while at Fr 0.3, it reaches 1.8 m. The highest wave elevation occurs at Fr 0.4 is 2 m, and it further increases to 2.5 m at Fr 0.5. Furthermore, at Fr 0.6 and 0.7, the highest wave elevations are 2.5 m and 3 m, respectively. Notably, the colours on the graph represent various transverse wave patterns, and their number decreases as the ship's speed increases. At Fr 0.3, a transverse wave with half the hull length occurs, characterized by wave crests in the midship area. Larger peak waves originate from the bow of the hull, leading to relatively larger waves. At Fr 0.4, where the highest wave is 2 m, the transverse wavelength matches the ship's hull length, and the interaction of waves at the front and back strengthens each other. In the context of Fr 0.6 and 0.7, with wave elevations of 2.5 and 3 m, respectively, different wave patterns emerge below the deck due to varying hull spacings. Notably, in this specific Froude number range, larger waves develop at the bow due to interaction effects resulting from specific hull spacing and speeds, potentially reducing wave resistance.

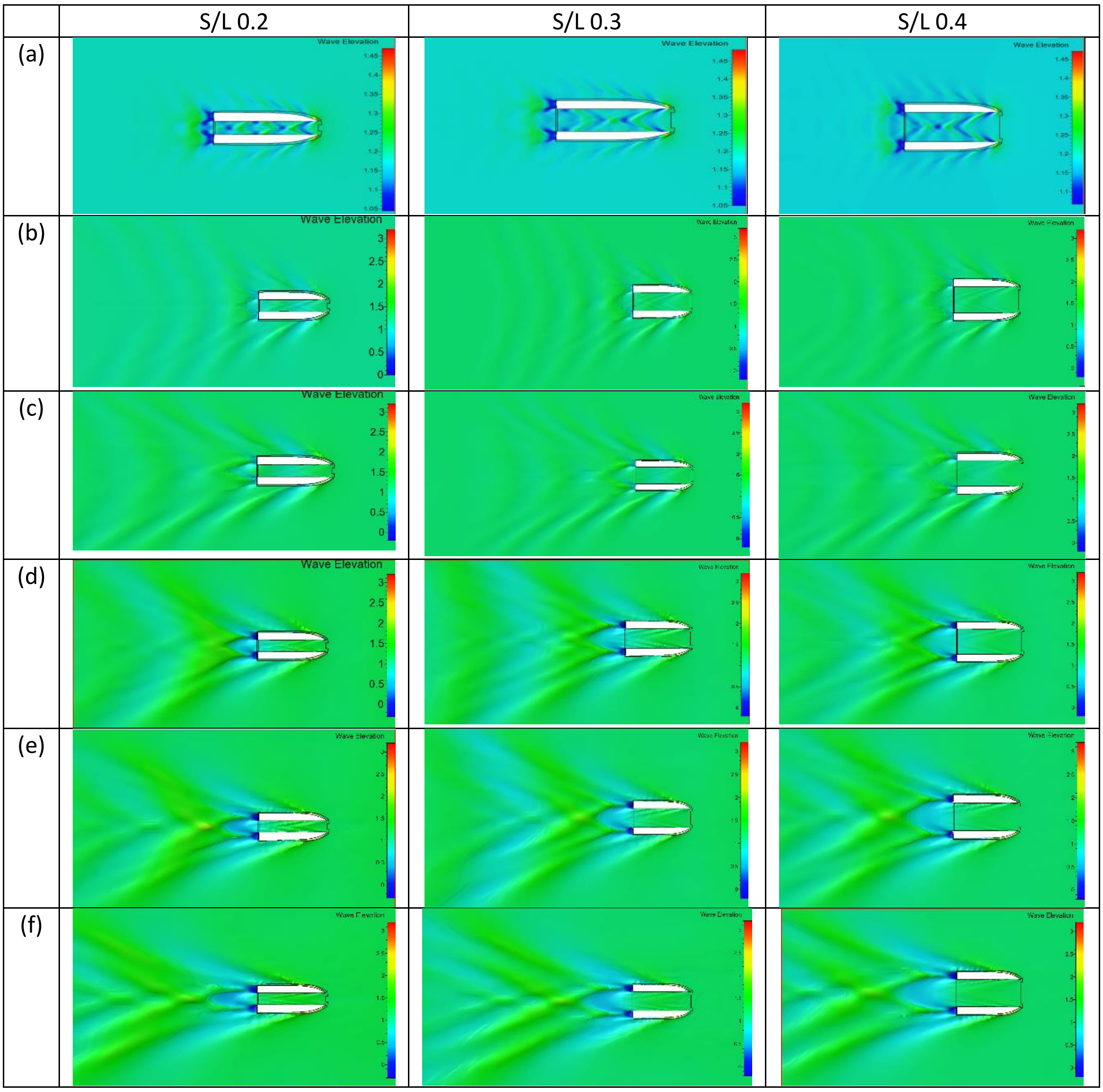

Fig. 5. Wave Elevation Contour in (a) Fr 0.2, (b) Fr 0.3, (c) Fr 0.4, (d) Fr 0.5, (e) Fr 0.6, (f) Fr 0.7 with S/L 0.2-0.4

The result of the resistance coefficient in the different hull spacing and Froude number are shown in Figure 6 to Figure 8. Figure 6 illustrates the variations in total resistance (C_T), friction resistance (C_F), wave resistance (Cw), and viscous resistance (Cv) concerning S/L at a value of 0.2. Notably, Cw and C_T exhibit the same trend, reaching its peak values at Fr 0.5, with CT generate maximum value of 17.45 x 10^{-3} and Cw at 13.95 x 10^{-3}. Meanwhile, CF and Cv exhibit a similar pattern at S/L 0.2 but demonstrate different behavior across various Froude Numbers. The highest recorded value for CF is 2.13 x 10^{-3} and for Cv, it stands at 3.5 x 10^{-3}. It is noteworthy that at S/L 0.2, the data signifies peak resistance at a Froude Number of 0.5. Furthermore, it is observed that as the Froude Number escalates from 0.2 to 0.5, vessel speed correlates with an increase in resistance. This is caused by an increase in speed affecting resistance, where resistance decreases as speed increases (expressed as the Froude number) [18]. However, in the Fr range of 0.6-0.7, the trend reverses, showing a decrease in resistance as speed rises. This is due to the onset of wave breaking and spray occurring at Fr values above 0.5 [19].

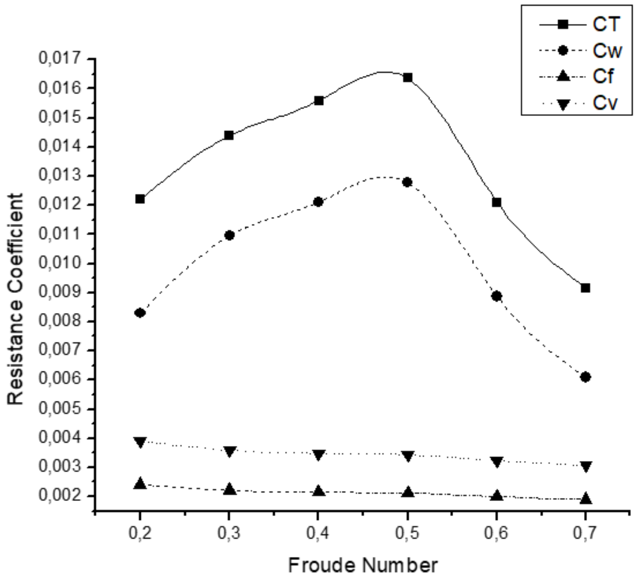

Fig. 6. Component of resistance S/L 0.2 in different Froude number

Figure 7 shows the total resistance (C_T), friction resistance (C_F), wave resistance (Cw), and viscous resistance (Cv) of the 0.3 ship hull spacing variation. Notably, Cw and C_T exhibit similar trend, with their peak values occurring at a Fr 0.5. At this Fr value, C_T attains its maximum at 16.59 x 10^{-3}, while Cw reaches 13.1 x 10^{-3}. Conversely, C_F and Cv display a consistent pattern at S/L 0.3 across various Fr, with the highest values at 2.14 x 10^{-3} for C_F and 3.49 x 10^{-3} for Cv. This phenomenon is a result of rising speed impacting resistance, with resistance diminishing as speed increases [17]. Nevertheless, in the Fr range of 0.6-0.7, this pattern shifts, demonstrating a decline in resistance with increasing speed. This alteration is attributed to the initiation of wave breaking and spray at Fr values exceeding 0.5 [21].

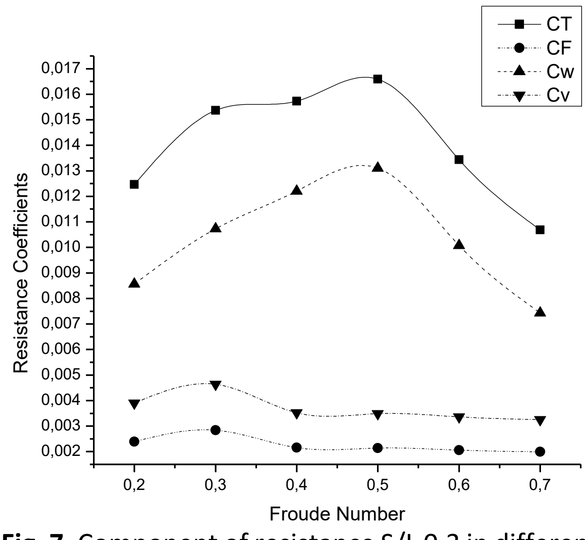

Fig. 7. Component of resistance S/L 0.3 in different Froude number

Figure 8 presents data on total resistance (C_T), friction resistance (C_F), wave resistance (Cw), and viscous resistance (Cv) at S/L 0.4. Similar trend of Cw and CT occured with their peak values at Fr 0.5. At this Fr value, C_T reaches its maximum at 16.36 x 10^{-3}, while Cw generates 12.77 x 10^{-3}. Similarly, C_F and Cv follow the same trend at S/L 0.4 across different Fr, with the highest values at 2.12 x 10-3 for C_F and 3.44 x 10^{-3} for Cv. It is important to highlight that at S/L 0.4, the data indicates the highest resistance values at a Froude Number of 0.5. The observed phenomenon is a consequence of heightened speed influencing resistance, resulting in a reduction in resistance as speed escalates, a relationship expressed through the Froude number [17]. However, within the Froude number range of 0.6-0.7, there is a notable reversal in this pattern, where resistance decreases as speed increases. This shift can be attributed to the initiation of wave breaking and spray, which becomes prominent at Froude number values exceeding 0.5 [21].

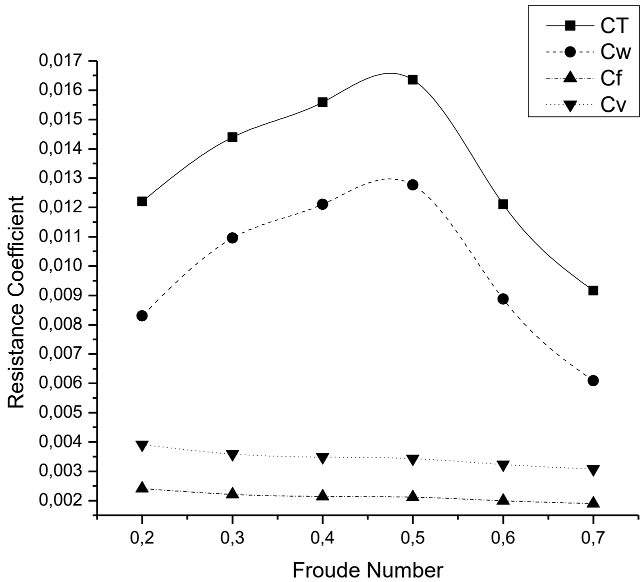

Fig. 8. Component of resistance S/L 0.4 in different Froude number

The phenomenon of viscous interference arises due to changes in the distribution of the boundary layer and the acceleration of flow velocity near a catamaran's hulls. It also results from the distribution of pressure changes in the area between the demihull. These phenomena are discussed through the study and simulation of CFD and calculate with Eq. (8). The value of the viscous form factor is influenced by the distance between the hulls (S/L) shown in Figure 9, expressing that as the distance between the hulls (S/L) increases, the initial value of the viscous form factor decreases. The value of viscous component factors is concluded in Table 3.

Table 3
Viscous Interference Factor

Fr	S/L 0,2	S/L 0,3	S/L 0,4
0.2	1.1002	1.0514	1.0156
0.3	1.1030	1.0483	1.0113
0.4	1.1044	1.0472	1.0116
0.5	1.1104	1.0449	1.0124
0.6	1.1052	1.0467	1.0157
0.7	1.1168	1.0483	1.0108

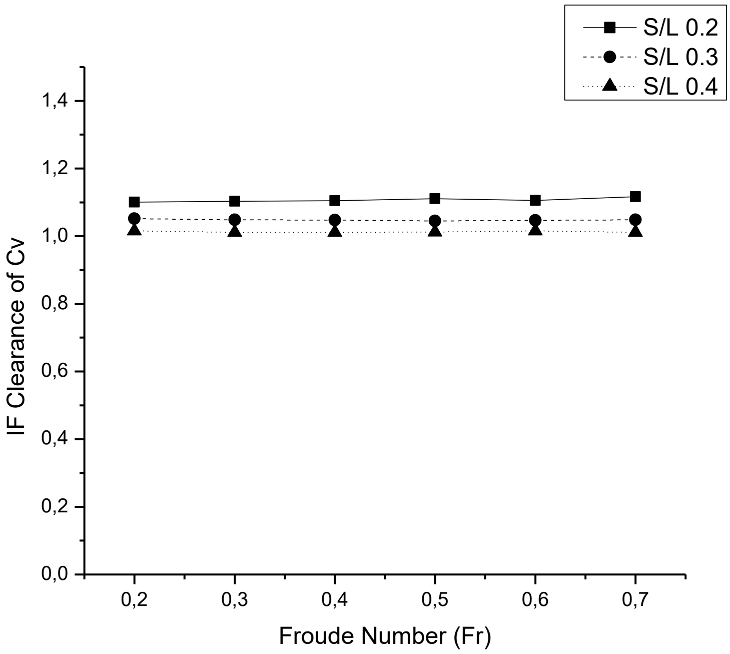

Fig. 9. Viscous interference factor in different hull spacing and Froude number

Wave interference factor calculated using Eq. (7). It is observed that fluctuations in clearance between the hulls were experienced across different Fr, as depicted in Figure 10 and summarized in Table 4. The effect of wave interference factor in S/L 0.2 in Fr. 0.3 and wave interference become smaller in Fr > 0.3. This was caused by a certain distance and speed generated by interaction effect waves which can negate each other, resulting in smaller wave resistance. The change in wave interference factor is also influenced by the variation in the distance between the hulls (S/L). The greater the distance between the hulls, the lower the pressure and wave elevation that occurred. This is because of disturbances in the flow velocity and pressure around the demi hulls, which increase, particularly in the inner area due to the interaction between hull and water surface [16,22,23].

Table 4
Wave Interference Factor (τ)

Fr	S/L 0,2	S/L 0,3	S/L 0,4
0.2	0.9748	0.8803	0.8748
0.3	1.1711	1.1278	0.9891
0.4	1.0300	0.9859	0.9840
0.5	1.1230	1.0162	0.9912
0.6	1.0462	1.0070	0.9964
0.7	0.9685	0.9441	0.9275

Pressure and flow velocity variations due to alterations in catamaran hull clearance were assessed via Computational Fluid Dynamics (CFD), and the outcomes are summarized in Table 5. Viscous interference was deconstructed into two essential factors: σ, responsible for accounting for velocity augmentation between the hulls, as observed in Figure 11(a), σ and ø, responsible for considering changes in the pressure field around the demihulls as shown in Figure 11(b). Significantly, it was observed that each of these factors remained constant across the Fr variations studied. Furthermore, as S/L decreased, the flow velocity ratio increased, intensifying the velocity between the hulls. In contrast, a contrasting trend was evident in the flow pressure ratio, as larger S/L resulted in smaller pressure ratios [23,24].

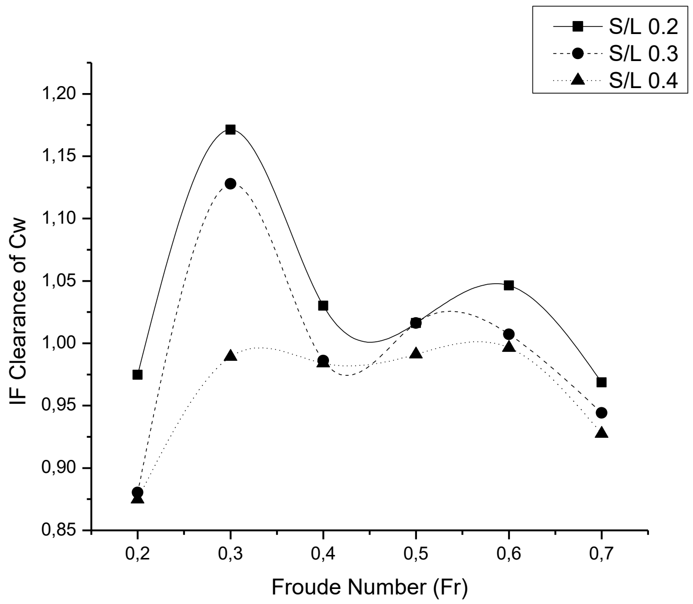

Fig. 10. Wave interference factor in different hull spacing and Froude number

Table 5
Interference of Flow Velocity (σ) and pressure (ø) from CFD results

Fr	Rn	Sc/L=0.2	Sc/L=0.3	Sc/L=0.4
		inner /outer		
Flow Velocity (σ)				
0.2	4.21×10^7	0.9921	0.9616	0.9289
0.3	6.73×10^7	0.9898	0.9596	0.9267
0.4	8.42×10^7	0.9879	0.9582	0.9255
0.5	1.09×10^8	0.9883	0.9591	0.9258
0.6	1.26×10^8	0.9885	0.9578	0.9240
0.7	1.52×10^8	0.9882	0.9560	0.9225
Flow Pressure (ø)				
0.2	4.21×10^7	1.2619	1.4066	1.5468
0.3	6.73×10^7	1.2666	1.4109	1.5441
0.4	8.42×10^7	1.2700	1.4117	1.5479
0.5	1.09×10^8	1.2702	1.4142	1.5522
0.6	1.26×10^8	1.2697	1.4220	1.5500
0.7	1.52×10^8	1.2707	1.4242	1.5433

The research findings of Insel and Molland [6] indicate that wave resistance interference has a positive effect on catamaran hulls within the Froude Number (Fr) range of 0.35 - 0.42. Furthermore, the results of the research by Broglia *et al.,* [13] shows similar phenomenon occurs within the Fr range of 0.2 to 0.4. Based on the research conducted through CFD simulations and calculations using Eq. (7) as depicted in Figure 12, it is indicated that the favourable impact of wave resistance interference on catamaran hulls is not confined to Froude (Fr) values below 0.4 but is also evident at Fr values exceeding 0.5.

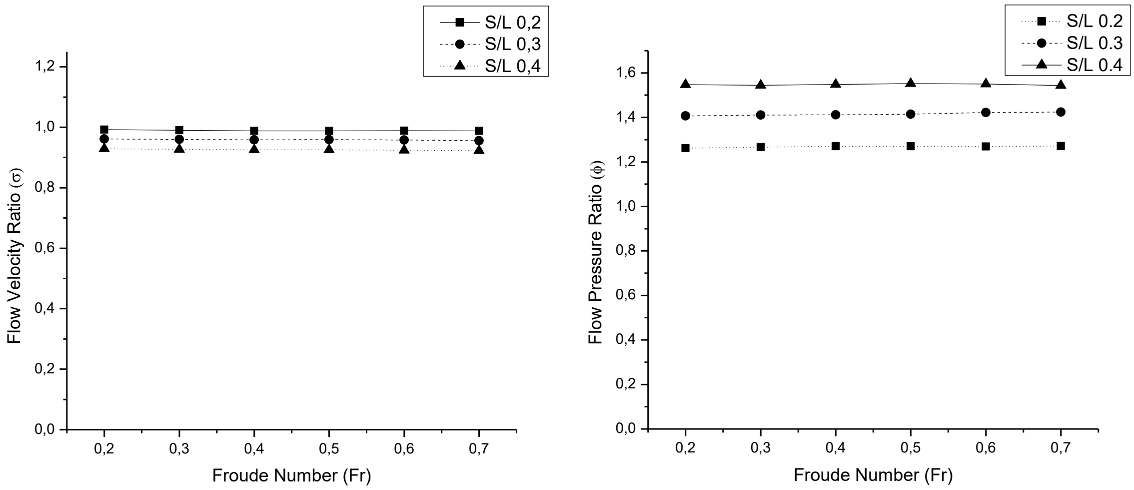

(a) (b)

Fig. 11. Viscous interference, σ, based on flow velocity (CFD result); (a) Flow velocity (σ), (b) Flow pressure (ø)

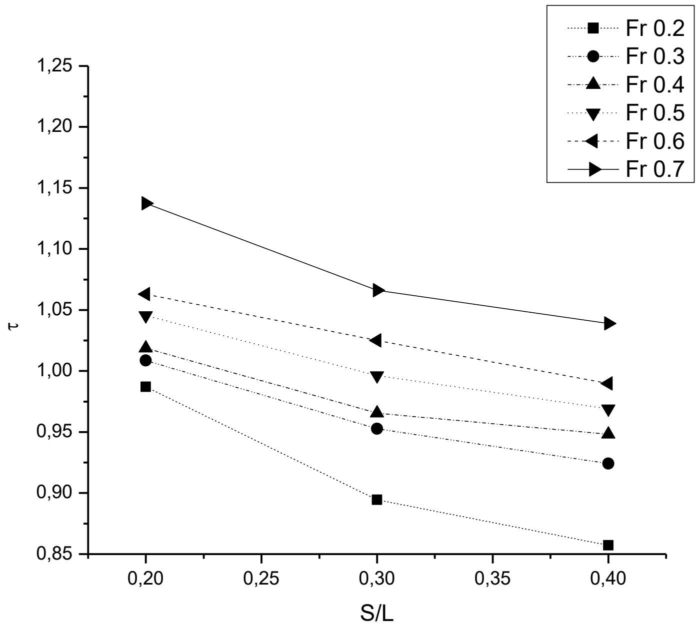

Fig. 12. Wave interference, τ, based on CFD result

Regression analysis was utilized provides interference factors (τ) a set of curves for various S/L. This approach leads to the derivation of equations for interference factors related to hull clearances/ Figure 13 visually represents these equations and demonstrates an intriguing trend: S/L increases, the value of τ consistently decreases [5,24].

Regression analysis was utilized to provides resistance components within a set of curves for different Froude Numbers (Fr) and flow pressure (ø) within a set of curves for various S/L. Figure 14 provides a clear illustration of the relationship between S/L and interference viscous resistance. As the hull clearance (the distance between the hulls) increases, there is a continuous and noticeable increase in the values associated with viscous resistance interference [5,24].

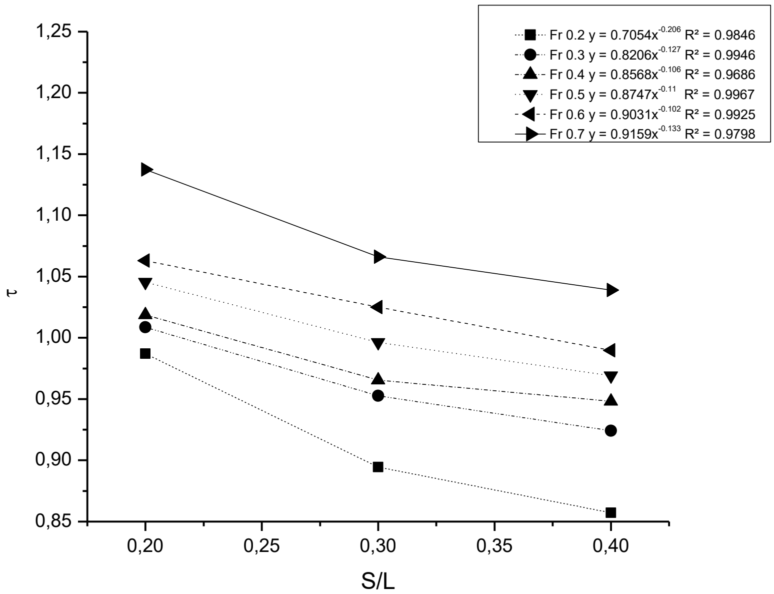

Fig. 13. Regression of wave resistance interference (τ)

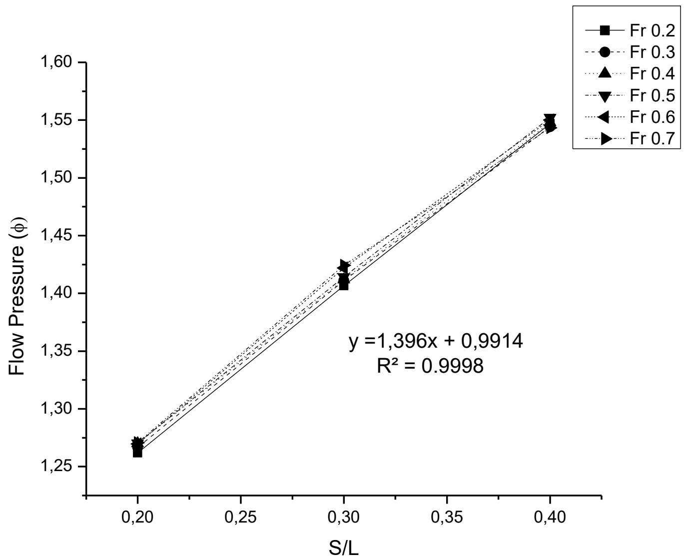

Fig. 14. Regression of viscous resistance interference (ø)

Regression analysis was employed to investigate resistance components within two sets of curves: one for different Froude Numbers (Fr) and the other for various ship length to waterline length ratios (S/L), specifically focusing on flow velocity (σ), as depicted in Figure 15. It is observed that the interference viscous resistance value remains consistent across different Froude Numbers, implying that it doesn't vary with changes in speed. However, what is particularly noteworthy is that this resistance value decreases as the S/L becomes larger. The regression model takes into consideration that a specific variable may follow linear, power, or exponential relationships, summarized in Table 6.

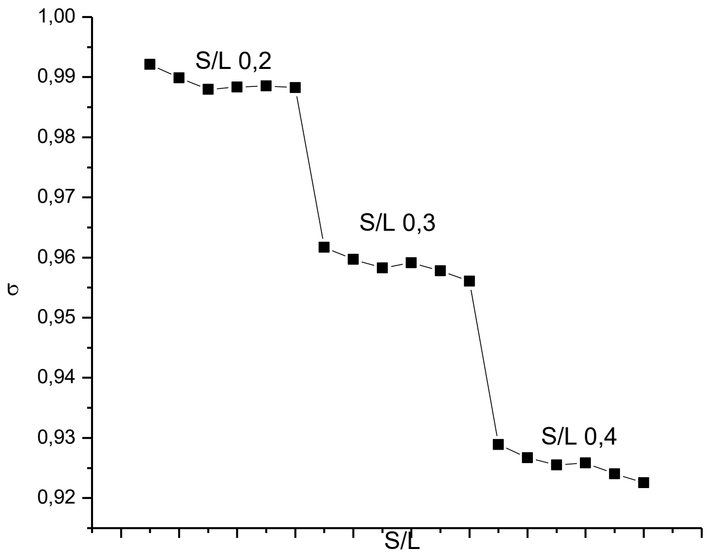

Fig. 15. Regression of viscous resistance interference (σ)

Table 6
Results of Regression Analysis

Symbol	Equation	Curve Form	Validity Factor (R^2)
τ (Fr 0.2)	$\tau = 0.7054(S/L)^{-0.206}$	Power	0.9846
τ (Fr 0.3)	$\tau = 0.8206(S/L)^{-0.127}$		0.9946
τ (Fr 0.4)	$\tau = 0.8568(S/L)^{-0.106}$		0.9686
τ (Fr 0.5)	$\tau = 0.8747(S/L)^{-0.11}$		0.9967
τ (Fr 0.6)	$\tau = 0.9031(S/L)^{-0.102}$		0.9925
τ (Fr 0.7)	$\tau = 0.9159(S/L)^{-0.133}$		0.9798
Ø	Ø =1.396 (S/L) + 0.9914	Linear	0.9998
σ	$\sigma = 1.0045e^{-0.005(S/L)}$	Exponential	0.9238

4. Conclusion

A successful combination of numerical optimization modeling and CFD simulations has been utilized to predict the optimal total resistance coefficient (C_T) for a catamaran hull. The numerical findings emphasize that changes in speed have a substantial effect on the resistance characteristics of catamarans, primarily due to interactions between the hulls, causing waves and viscosity effects. The largest resistance coefficient on S/L 0.2, 0.3, and 0.4 respectively are 17.45 x 10^{-3}, 16.59 x 10^{-3}, and 16.36 x 10^{-3}, which occurred at Fr 0.5.

The effect of wave interference factor in S/L 0.2 in Fr. 0.3 and wave interference become smaller in Fr > 0.3. This was caused by a certain distance and speed generated by interaction effect waves which can negate each other, resulting in wave resistance to be smaller. S/L is very crucial for the emergence of wave interactions (wave making) which impacting the wave effect between the demi hulls. The viscous interference factors are generating little differences for each S/L in Fr 0.2 to 0.7 because it has relatively no effect on speeds.

Regression technique was employed to analyze these variables ø, σ and τ. The regression analysis provides interference factors (τ) for resistance components in a set of curves for various Froude Numbers and viscous components (ø and σ) in a set of curves for different S/L. Consistent inverse trend for τ occurred as S/L increased, where the values consistently decreased. Interference viscous resistance of flow velocity σ remained constant across varying Froude Numbers, emphasizing its independence from speed alterations, yet exhibited a decrease as S/L increased. The resistance components were influenced by Froude Numbers and separation to length (S/L), with flow pressure ø showing a notable increase as hull clearances expanded.

Acknowledgment
The authors wished to thank the Institut Teknologi Sepuluh Nopember for funding the research through a research scheme known as "Research for Doctoral Dissertation" under contract numbers: 112/E5/PG.02.00.PL/2023 and 1902/PKS/ITS/2023.

References

[1] Moraes, H. B., J. M. Vasconcellos, and R. G. Latorre. "Wave resistance for high-speed catamarans." *Ocean Engineering* 31, no. 17-18 (2004): 2253-2282. https://doi.org/10.1016/j.oceaneng.2004.03.012
[2] Tuck, Ernest O. "Wave resistance of thin ships and catamarans." *Applied Mathematics Report T8701* (1987).
[3] Fang, Chih-Chung, and Hoi-Sang Chan. "An investigation on the vertical motion sickness characteristics of a high-speed catamaran ferry." *Ocean Engineering* 34, no. 14-15 (2007): 1909-1917. https://doi.org/10.1016/j.oceaneng.2007.04.001
[4] Molland, Anthony F., Stephen R. Turnock, and Dominic A. Hudson. *Ship resistance and propulsion*. Cambridge University Press, 2017. https://doi.org/10.1017/9781316494196
[5] Jamaluddin, A., I. K. A. P. Utama, B. Widodo, and A. F. Molland. "Experimental and numerical study of the resistance component interactions of catamarans." *Proceedings of the Institution of Mechanical Engineers, Part M: Journal of Engineering for the Maritime Environment* 227, no. 1 (2013): 51-60. https://doi.org/10.1177/1475090212451694
[6] Insel, M., and A. F. Molland. "An investigation into the resistance components of high speed displacement catamarans." *Transactions of The Royal Institution of Naval Architects, RINA* 133 (1991).
[7] Luhulima, Richard Benny, I. K. A. P. Utama, Bagiyo Suwasono, and Sutiyo Sutiyo. "CFD Analysis into the Correlation between Resistance and Seakeeping of Trimaran Configuration." In *Proceeding of Marine Safety and Maritime Installation (MSMI 2018)*, pp. 338-348. 2018.
[8] Nair, Vinod V., and S. K. Bhattacharyya. "Water entry and exit of axisymmetric bodies by CFD approach." *Journal of Ocean Engineering and Science* 3, no. 2 (2018): 156-174. https://doi.org/10.1016/j.joes.2018.05.002
[9] He, Wei, Teresa Castiglione, Manivannan Kandasamy, and Frederick Stern. "Numerical analysis of the interference effects on resistance, sinkage and trim of a fast catamaran." *Journal of Marine Science and Technology* 20 (2015): 292-308. https://doi.org/10.1007/s00773-014-0283-0
[10] Sadeghi, Mohamad, and Ahmad Hajivand. "Investigation the effect of canted rudder on the roll damping of a twin-rudder ship." *Applied Ocean Research* 103 (2020): 102324. https://doi.org/10.1016/j.apor.2020.102324
[11] Sadeghi, Mohamad, and Hamid Zeraatgar. "Investigation on the effect of anti-pitch fins for reducing the motion and acceleration of ships using computational fluid dynamics." *Ocean Engineering* 267 (2023): 112965. https://doi.org/10.1016/j.oceaneng.2022.112965
[12] Menter, Florian R. "Performance of popular turbulence model for attached and separated adverse pressure gradient flows." *AIAA Journal* 30, no. 8 (1992): 2066-2072. https://doi.org/10.2514/3.11180
[13] Broglia, Riccardo, Boris Jacob, Stefano Zaghi, Frederick Stern, and Angelo Olivieri. "Experimental investigation of interference effects for high-speed catamarans." *Ocean Engineering* 76 (2014): 75-85. https://doi.org/10.1016/j.oceaneng.2013.12.003
[14] Fitriadhy, Ahmad, Nurul Shukna Rizat, Atiyah Raihanah Abd Razak, Sheikh Fakhruradzi Abdullah, Faisal Mahmuddin, and Alamsyah Kurniawan. "Optimization Modelling of a Catamaran Hull Form towards Reducing Ship's Total Resistance." *CFD Letters* 14, no. 4 (2022): 67-79. https://doi.org/10.37934/cfdl.14.4.6779
[15] Anderson, John David, and John Wendt. *Computational fluid dynamics*. Vol. 206. New York: McGraw-hill, 1995.
[16] Zhou, Peng, Liwei Liu, Lixiang Guo, Qing Wang, and Xianzhou Wang. "Numerical Study on the Effect of Stern Flap for Hydrodynamic Performance of Catamaran." In *International Conference on Offshore Mechanics and Arctic Engineering*, vol. 58776, p. V002T08A056. American Society of Mechanical Engineers, 2019. https://doi.org/10.1115/OMAE2019-96819
[17] Liu, Zhaochun, Xiufeng Zhang, Yao Meng, and Linghong Wang. "Numerical calculation of the resistance of catamarans at different distances between two hulls." In *E3S Web of Conferences*, vol. 283, p. 01008. EDP Sciences, 2021. https://doi.org/10.1051/e3sconf/202128301008
[18] Fitriadhy, Ahmad, Intan Nur Nabila, Christina Bangi Grosnin, Faisal Mahmuddin, and Suandar Baso. "Computational Investigation into Prediction of Lift Force and Resistance of a Hydrofoil Ship." *CFD Letters* 14, no. 4 (2022): 51-66. https://doi.org/10.37934/cfdl.14.4.5166

[19] Wulandari, Amalia Ika, Mukhtar Prabu Dewanagara, Muhammad Uswah Pawara, and Syerly Klara. "Comparative Study of Rudder Performance of Single Plate and Fishtail of SPOB Ship Using CFD Method." *CFD Letters* 14, no. 5 (2022): 43-55. https://doi.org/10.37934/cfdl.14.5.4355

[20] Suastika, Ketut, Gilbert Ebenezer Nadapdap, Muhammad Hafiz Nurwahyu Aliffrananda, Yuda Apri Hermawan, I. Ketut Aria Pria Utama, and Wasis Dwi Aryawan. "Resistance analysis of a hydrofoil supported watercraft (Hysuwac): a case study." *CFD Letters* 14, no. 1 (2022): 87-98. https://doi.org/10.37934/cfdl.14.1.8798

[21] Resistance Committee. *ITTC-Recommended Procedures. Uncertainty Analysis in CFD, Examples for Resistance and Flow*. International Towing Tank Conference. 7.5-03-02-01. 1999.

[22] Li, Mingxin, Yi Chen, Zhi-Ming Yuan, Yong Cheng, and Longbin Tao. "Interference effects on the upstream wave generated by the catamaran moving across a depth change." *Ocean Engineering* 287 (2023): 115939. https://doi.org/10.1016/j.oceaneng.2023.115939

[23] Jamaluddin, Andi. "Wave Pattern dan Interaksi Hambatan Gelombang pada Kapal Lambung Ganda (Twin Hull): Kajian Analisa Numerik." *Wave: Jurnal Ilmiah Teknologi Maritim* 4, no. 1 (2010): 6-11. https://doi.org/10.29122/jurnalwave.v4i1.3541

[24] Van't Veer, A. P., and F. R. T. Siregar. "The interaction effects on a catamaran travelling with forward speed in waves." In *Proceedings of the Third International Reference on Fast Sea Transportation, FAST'95*, pp. 87-98. 1995.